


Variation in the sediment deposition behind check-dams under different soil erosion conditions on the Loess Plateau, China

Yanhong Wei,^{1,3}  Zhong He,^{1,2} Juying Jiao,^{1,2*} Yujin Li,² Yixian Chen¹ and Hengkang Zhao²

¹ State Key Laboratory of Soil Erosion and Dryland Farming on Loess Plateau, Institute of Soil and Water Conservation, Chinese Academy of Sciences and Ministry of Water Resources, Yangling, Shaanxi Province, China

² Institute of Soil and Water Conservation, Northwest A&F University, Yangling, Shaanxi Province, China

³ Key Laboratory of Desert and Desertification, Northwest Institute of Eco-Environment and Resources, Chinese Academy of Sciences, Lanzhou, Gansu Province, China

Received 5 March 2017; Revised 1 February 2018; Accepted 8 February 2018

*Correspondence to: Juying Jiao, Institute of Soil and Water Conservation, Northwest A&F University, No. 26, Xingong Road, Yangling, Shaanxi, 712100, China. E-mail: jyjiao@ms.iswc.ac.cn

ESPL

Earth Surface Processes and Landforms

ABSTRACT: To maintain a reasonable sediment regulation system in the middle reaches of the Yellow River, it is critical to determine the variation in sediment deposition behind check-dams for different soil erosion conditions. Sediment samples were collected by using a drilling machine in the Fangta watershed of the loess hilly–gully region and the Manhonggou watershed of the weathered sandstone hilly–gully (*pisha*) region. On the basis of the check-dam capacity curves, the soil bulk densities and the couplet thickness in these two small watersheds, the sediment yields were deduced at the watershed scale. The annual average sediment deposition rate in the Manhonggou watershed (702.0 mm/(km²·a)) from 1976 to 2009 was much higher than that in the Fangta watershed (171.6 mm/(km²·a)) from 1975 to 2013. The soil particle size distributions in these two small watersheds were generally centred on the silt and sand fractions, which were 42.4% and 50.7% in the Fangta watershed and 60.6% and 32.9% in the Manhonggou watershed, respectively. The annual sediment deposition yield exhibited a decreasing trend; the transition years were 1991 in the Fangta watershed and 1996 in the Manhonggou watershed ($P < 0.05$). In contrast, the annual average sediment deposition yield was much higher in the Manhonggou watershed (14011.1 t/(km²·a)) than in the Fangta watershed (3149.6 t/(km²·a)). In addition, the rainfalls that induced sediment deposition at the check-dams were greater than 30 mm in the Fangta watershed and 20 mm in the Manhonggou watershed. The rainfall was not the main reason for the difference in the sediment yield between the two small watersheds. The conversion of farmland to forestland or grassland was the main reason for the decrease in the soil erosion in the Fangta watershed, while the weathered sandstone and bare land were the main factors driving the high sediment yield in the Manhonggou watershed. Knowledge of the sediment deposition process of check-dams and the variation in the catchment sediment yield under different soil erosion conditions can serve as a basis for the implementation of improved soil erosion and sediment control strategies, particularly in semi-arid hilly–gully regions. Copyright © 2018 John Wiley & Sons, Ltd.

KEYWORDS: dam-controlled watershed; sedimentation; erosion environment; sediment yield; sediment particle size; the Loess Plateau

Introduction

Soil erosion and both its on-site and off-site impacts are increasingly seen as a major environmental problem across the world (Porto *et al.*, 2014). Severe soil erosion has led to the loss of approximately 10 million hectares of cropland per year worldwide, not only reducing the cultivable land for food production but also causing land degradation and river siltation (Onyando *et al.*, 2005; Pimentel, 2006). The Chinese Loess Plateau, located in the middle reaches of the Yellow River, is one of the most severe soil and water loss areas in the world; more than 60% of the land has been subjected to intense soil erosion with an intensity of 2000 to 20000 t/(km²·a), causing riverbed uplift (3–8 m) and flood disasters in the lower Yellow River (Fu, 1989; Shi and Shao, 2000; Xin *et al.*, 2012). Soil erosion involves the processes of detachment, transport and deposition of soil

materials by erosive rainfalls and runoff (Shi *et al.*, 2012). Among these processes, the soil materials and sediment transport depends on both the sediment properties and hydraulic parameters of the flow (Sui *et al.*, 2009). The sediment particle shape affects the incipient motion of the sediment (Wang and Ditttrich, 1999), while the hydraulic parameters of the flow influence the sediment transport capacity and river dynamics (Wang and Wu, 2001). As a result, the grain size distribution of sediment has long been used as an indicator of sediment availability, flow competency and transport mechanism (Beierle *et al.*, 2002). Sediment size distribution greatly affects sediment transport and deposition (Shi *et al.*, 2012). Xu *et al.* (2009a) analysed the correlation coefficient between channel sedimentation and sediment input and found that it increases with the grain size, indicating that channel sedimentation depended more on coarser grain size fractions than on smaller ones and that for the grain sizes of sediment

input > 0.05 mm and > 0.10 mm, 76.61% and 97.68% were deposited on the channel, respectively. Once sediment particles are delivered to streams, rivers and lakes, sedimentation will be a major problem in the watershed (Pham *et al.*, 2001). Sediment is a combination of primary soil particles (sand, silt and clay) and secondary or aggregated soil material (Mitchell *et al.*, 1983). Sediment transfer from continents to oceans via rivers is an important component of sediment recycling in earth systems and contributes 95% of the sediment entering the ocean (Syvitski, 2003; Chakrapani, 2005). Milliman and Syvitski (1992) estimated that the global sediment load into the sea reached 200×10^8 t annually. The existing research results indicate that sediment transport by rivers has generally decreased globally following reservoir and check-dam construction and sediment loss due to water abstraction and land use change in recent years (Khafagy *et al.*, 1992; Carriquiry and Sánchez, 1999; Mikhailova, 2003; Walling and Fang, 2003; Wang *et al.*, 2007; Liu *et al.*, 2008).

Soil and water loss in the Chinese Loess Plateau has greatly depleted land resources and degraded the eco-environment. This rolling plateau is characterized by a large area and complex geomorphology, and it can be divided into two geomorphologic units: in the gully area (gully slopes), gully erosion and mass movement are predominant, and in the inter-gully area (hillslopes), land has been extensively cultivated, causing widespread sheet and rill erosion (Feng *et al.*, 2003; Xu *et al.*, 2009b). The relative sediment contributions in a small watershed of the loess hilly region from the inter-gully area and from the gully area are approximately 24–40% and 60–76%, respectively (Jing, 1986; Xu, 1987; Jiao *et al.*, 1992; Wen *et al.*, 1998; Feng *et al.*, 2003; Yang *et al.*, 2006). Li *et al.* (2003) indicated that the rill and gully erosion are the dominant water erosion processes and contribute 60–90% of the total sediment production in a small watershed of the Chinese Loess Plateau. Numerous studies conducted in China and abroad indicate that gully erosion is often the main source of sediment in small watersheds (Jiao *et al.*, 1992; Wasson *et al.*, 2002; Krause *et al.*, 2003; de Vente *et al.*, 2005; Yang *et al.*, 2006; Chen *et al.*, 2016). Gully erosion is most often triggered or accelerated by a combination of inappropriate land use and extreme rainfall events, so many gullies are required to capture sediment and reduce soil erosion (Valentin *et al.*, 2005). In the Chinese Loess Plateau, many years of soil and water conservation has demonstrated that check-dams are effective measures to control gully erosion (Xu *et al.*, 2009b; Xin *et al.*, 2012). Moreover, the check-dams not only considerably reduced the stream bed slopes but also caused a disruption in the connectivity of the rivers and diminished their capacity to transport sediment (Díaz *et al.*, 2014). Approximately 110 thousand check-dams have been built in the small watersheds of the Loess Plateau over the past 50 years, and approximately 21 billion m^3 of sediments have been captured by these dams (Jin *et al.*, 2012). In the Yanhe watershed, the annual runoff was reduced by less than 14.3% due to the check-dams in the gullies, while up to 85.5% of the sediment was retained during the rainy season (Xu *et al.*, 2013). Check-dams in a small gully basin of India played a very important role and reduced the sediment yield by 41.5% through trapping sediment and reducing erosion (Shit *et al.*, 2013).

Generally, a small watershed is treated as a planning and construction unit for check-dams (Wang *et al.*, 2011b). Sediments intercepted by a check-dam are an important source of information to estimate the soil erosion and sediment yield at the scale of a small watershed because check-dams trap most of the sediments produced from the catchments (Wang *et al.*, 2014; Ramos-Diez *et al.*, 2016b). Understanding the soil erosion and deposition rates in a small watershed is of vital importance for designing soil and water conservation measures

and river basin management plans (Li *et al.*, 2009; Suif *et al.*, 2016; Tian *et al.*, 2013). At present, estimation of the sediment yield of small watersheds based on the sediment trapped by check-dams is becoming a research hotspot (Ramos-Diez *et al.*, 2016a). Accurate estimation of sediment yield from small watersheds contributes to a better understanding of the linkage between soil erosion processes on hillslopes and sediment transport in rivers (Verstraeten and Poesen, 2001). Meanwhile, the effectiveness of check-dams in trapping sediment is associated with the remaining capacity of the check-dams, while the variation in the sediment yield in small watersheds is associated with large differences in the erosive rainfall, catchment area, vegetation cover, slope steepness, soil erodibility factor, and other factors (Vaezi *et al.*, 2017). Therefore, to decrease catchment sediment yield, the combination of vegetation measures and check-dams engineering measures can be used to control gully erosion and sediment transport effectively in areas with high erodibility, particularly in the semi-arid hilly–gully regions of the Loess Plateau (Yan *et al.*, 2015). Furthermore, our results are more likely to accurately estimate erosion rates and sediment yields in small watersheds under different soil erosion conditions, thus leading to a better understanding of the effects of check-dams on fragile ecological environment restoration in the semi-arid hilly–gully regions. In general, the main objectives of this research were to (1) determine the variations in sediment deposition rate, sediment particle size and sediment deposition yield at the small watershed scale, (2) compare the difference in sediment deposition under different soil erosion conditions and (3) analyse the main factors influencing sediment deposition in two small watersheds. These small watersheds belong to the loess hilly–gully region but vary in geology and soil texture. Learning about the sediment deposition process of check-dams and the variation in catchment sediment yield under different soil erosion conditions can serve as a basis for implementing improved soil erosion and sediment control strategies, particularly in semi-arid hilly–gully regions.

Materials and Methods

Study area

The Yanhe and Huangfuchuan tributaries are first-order tributaries of the middle reaches of the Yellow River basin (Figure 1) and cover areas of 7725 km^2 and 3246 km^2 , respectively. Both watersheds are in a typical continental climate. The mean annual precipitation is 505 mm in the Yanhe watershed and 380 mm in the Huangfuchuan watershed. The mean annual temperatures are 8.8°C and 7.5°C, respectively (Xu *et al.*, 2013; Zhao *et al.*, 2015). The underlying surface conditions and soil types in the two watersheds are very different. In the Yanhe watershed, the landform is a typical loess hilly–gully landscape, and the loess covering 86.4% of the watershed is derived from loess parent material, which is a windblown under-consolidated deposit that formed over the past 2.5 million years in arid and semi-arid climatic conditions and is very erodible due to its macropores, well-developed vertical jointing and susceptibility to collapse on wetting (Zhang and Liu, 2010; Xu *et al.*, 2012). This region experiences intense soil erosion as a result of unreasonable land use management, low vegetation cover, erodible soils, and frequent high-intensity summer storms (Gao *et al.*, 2015). The annual sediment transport modulus at the Ganguyi hydrological station (Figure 1, the upstream area is 5852 km^2) ranged from 136.7 t/km^2 to 31100.5 t/km^2 with an average of 6728.3 $t/(km^2 \cdot a)$ from 1955 to 2014 (YRCC, 2014). However,

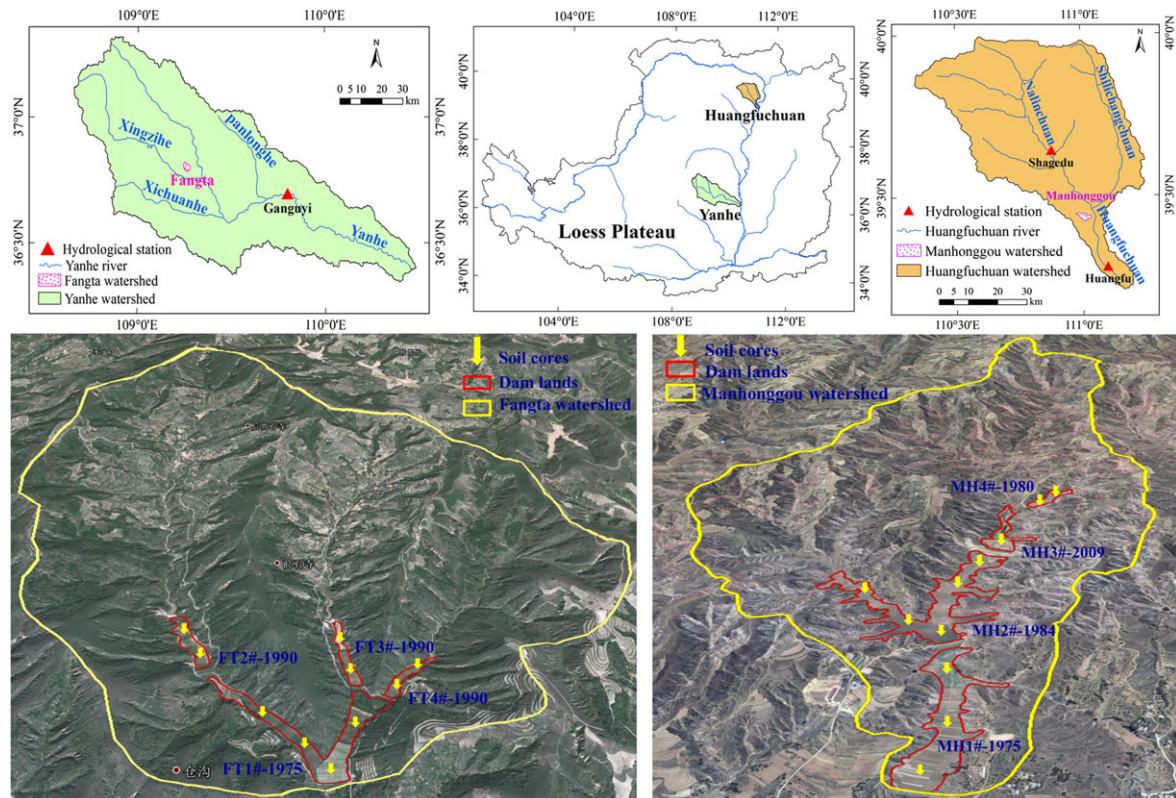


Figure 1. Location of the two studied areas and the selected check-dams. [Colour figure can be viewed at wileyonlinelibrary.com]

the landscape in the Huangfuchuan watershed includes a weathered sandstone hilly–gully region, extremely low (<20%) vegetation coverage and widely exposed bedrock (Linag *et al.*, 2017). The soil types are characterized by weathering sandstone, loess, and desert sand, and the land surface is dominated by dense gullies with poor vegetation cover (Wang *et al.*, 2012). In China, weathering sandstone (locally called *pisha* sandstone) is a general appellation for some types of fluvial clastic deposition sandstones and specifically refers to an interbedded rock consisting of Paleozoic Permian (approximately 2.5 hundred million years), Mesozoic Triassic, Jurassic and Cretaceous thick sandstone, sand shale and argillaceous sandstone (Ni *et al.*, 2008; Wei *et al.*, 2017). Although the area of *pisha* sandstone only accounts for 2.6% of the total Loess Plateau area, its coarse sediment yield accounts for 30% of the total coarse sediment in the upper–middle reaches of the Yellow River (Yang *et al.*, 2013). The frequently occurring storms, local topography, sparse vegetation and weathering sandstone have led to severe soil erosion in the basin (Zuo *et al.*, 2016). The annual average sediment yield at the Huangfu gauging station (Figure 1, the upstream area is 3199 km²) was between 0 t/km² and 53454.2 t/km² with an average of 12011.3 t/(km²·a) from 1955 to 2014 (YRCC, 2014).

Selection of typical small watersheds

Owing to the significant difference in the soil erosion characteristics and the systemic field investigations in the Yanhe and Huangfuchuan tributaries, two small watersheds located in the middle reaches of the Yellow River basin were selected for drilling because neither has been disturbed since formation (Figure 1): the Fangta dam-controlled watershed (36°47′19″–36°49′35″N, 109°14′40″–109°17′09″E) located in the Yanhe tributary and the Manhonggou dam-controlled watershed

(39°25′09″–39°26′43″N, 110°58′30″–111°02′14″E) located in the Huangfuchuan tributary.

The Fangta watershed is in the loess hilly–gully region at an altitude between 1100 m and 1350 m and is located in the upper and middle reaches of the Yanhe tributary, while the Manhonggou watershed is in the weathered sandstone (*pisha*) hilly–gully region at an altitude between 915 m and 1150 m and is located within the lower reaches of the Huangfuchuan tributary; these watersheds cover a drainage area of 8.4 km² and 6.8 km², respectively. The slopes in the Fangta and the Manhonggou watersheds are mostly 8–25° and 15–45°, accounting for 77.2% and 78.4% of the entire watershed, respectively. The land surface is characterized by dense gullies, with a gully density of 3.8 km/km² in the Fangta watershed and 4.3 km/km² in the Manhonggou watershed. The check-dams were constructed one by one from downstream to upstream in both watersheds to control soil erosion. The basic information on the check-dams for the Fangta watershed in the loess hilly–gully region and Manhonggou watershed in the weathered sandstone (*pisha*) hilly–gully region is shown in Table I.

Field sampling and measurement

Sediment samples were collected in the Fangta and Manhonggou watersheds using a drilling machine in May of 2014. In total, 10 soil cores were collected among the check-dams from the downstream to the upstream in the Fangta watershed at drilling depths between 6.01 m and 18.32 m, and 11 soil cores were similarly collected in the Manhonggou watershed at drilling depths between 10.37 m and 17.28 m. There were 5, 2, 2 and 1 sediment deposition cores at dams FT1#, FT2#, FT3# and FT4# in the Fangta watershed, and the 3, 5, 1 and 2 sediment deposition cores were collected at dams MH1#, MH2#, MH3# and MH4# in the Manhonggou watershed, respectively. All the sediment samples were cut in two

Table I. Basic information of check-dams in the Fangta and Manhonggou watersheds

Small watershed	Dam	Performance period	Deposition years	Watershed area (km ²)	Height (m)	Dam type	Utilization	Siltation
Fangta	FT1#	1975-1989	15	8.40	26	Large scale	Cultivation	Totally silted
	FT2#	1990-2008	19	4.00	24	Large scale	Unutilized	Partially silted
	FT3#	1990-2009	20	2.10	17	Medium scale	Unutilized	Partially silted
	FT4#	1990-2013	24	1.72	18	Medium scale	Unutilized	Partially silted
Manhonggou	MH1#	1976-1984	9	6.78	25	Large scale	Cultivation	Totally silted
	MH2#	1985-2007	23	6.10	22	Large scale	Cultivation	Totally silted
	MH3#	2009-2014	6	3.55	18	Large scale	Aquaculture	Partially silted
	MH4#	1981-2009	29	0.32	11	Small scale	Cultivation	Totally silted

halves; one half was preserved, and the other was used for hierarchical classification and sample collection. Finally, a total of 444, 208, 254 and 100 sediment samples from dams FT1#, FT2#, FT3# and FT4# and 452, 1016, 117 and 374 sediment samples from dams MH1#, MH2#, MH3# and MH4# were collected from the deposition profile. To determine the sediment particle size distribution, all the sediment samples were air-dried, and the rhizomes or gravels were removed. Then, the samples were crushed and passed through a 2-mm mesh sieve. The particle size distribution of the sediment samples was analysed using a Mastersizer 2000 laser particle size analyser (Malvern Instruments, Malvern, England) with a measurement interval ranging from 0.02 to 2000 μm . A soil cylinder with a volume of 100 cm³ was used for sampling to measure the soil bulk density to obtain the sediment deposition yield. Here, it should be stated that dam MH3# was not used in the analysis of this study because it contained water in the front and had a road and trees in the middle, and the deposition sequence was confusing.

The average elevation of the sediment surface and the silt area of all the selected check-dams were measured by means of a topographical survey employing a Total Station with an accuracy of ± 1 cm. First, we vectorized the early topography map (1:10,000) to establish the capacity curve of the check-dams. Second, the flood couplets were interpreted according to the thickness of the deposition layers, distribution of the sediment particle size and historical rainfall events. Then, the amount of sediment deposition was estimated based on the capacity curve, the soil bulk density and the thickness of the couplets. Finally, the sediment deposition rate and sediment deposition yield were obtained from the sediment deposition thickness and the mass of the couplets divided by its controlled watershed area, respectively. More details of these methods were described in Wei *et al.* (2017).

Statistical analysis

Since a severe rainstorm in the Chinese Loess Plateau could result in more sediment deposited behind the check-dams and vice versa (Li and Wei, 2011), we selected the erosive rainfall events with daily precipitation ≥ 12 mm (Xie *et al.*, 2000). Meanwhile, the Mann–Kendall nonparametric test (Mann, 1945; Kendall, 1975) was used to test the temporal trend in the annual sediment deposition rate and annual sediment yield time series, while the Pettitt test (Pettitt, 1979) was applied to identify the turning points in the annual sediment yield in the Fangta and Manhonggou watersheds. Significant differences in the annual deposition rate, sediment particle size and sediment deposition yield were detected using the independent samples t-test ($P < 0.05$), and the statistical determination was made using SPSS 17.0 software (SPSS Inc., 2008).

Results

Sediment deposition rate

According to the Mann–Kendall trend test, the annual sediment deposition rate showed a decreasing trend with increasing time at dams FT1#, FT2#, FT3# and FT4# of the loess hilly-gully region (statistic $Z < 0$). The annual average sediment deposition rate was 139.9 mm/(km²·a) at dam FT1# from 1975 to 1989, 152.0 mm/(km²·a) at dam FT2# from 1990 to 2008, 225.7 mm/(km²·a) at dam FT3# from 1990 to 2009, and 208.3 mm/(km²·a) at dam FT4# from 1990 to 2013. The highest and the lowest sediment deposition rates occurred at dam FT4#: the highest rate was 1336.2 mm/(km²·a) in 1990, and the lowest rate was 7.0 mm/(km²·a) in 2003 (Figure 2).

For the Manhonggou dam-controlled watershed in the weathered sandstone (*pisha*) region, the annual sediment deposition rate also exhibited a decreasing trend at dams MH1#, MH2# and MH4# (statistic $Z < 0$). The annual average sediment deposition rates were 290.3 mm/(km²·a) at dam MH1# from 1976 to 1984, 87.6 mm/(km²·a) at dam MH2# from 1985 to 2007, and 1488.0 mm/(km²·a) at dam MH4# from 1981 to 2009. The highest sediment deposition rate occurred in dam MH4# in 1982 at a rate of 4545.8 mm/(km²·a), while the lowest sediment deposition rate occurred at dam MH2# in 2000 at a rate of 10.9 mm/(km²·a) (Figure 3).

In Figure 4, the annual average sediment deposition rates differed significantly between the two small watersheds, and the annual average sediment deposition rate in the Manhonggou watershed (702.0 mm/(km²·a)) from 1976 to 2009 was much higher than in the Fangta watershed (171.6 mm/(km²·a)) from 1975 to 2013. On the basis of the box plot and the distribution curve, the height of the quartile box for the Manhonggou watershed was higher than that for the Fangta watershed. It was shown that the variation in the annual sediment deposition rate in the Manhonggou watershed was unstable, and the data points were scattered, while the Fangta watershed data were relatively stable and concentrated. Table II shows the independent samples t-test of the annual sediment deposition rate; the probabilities of the F-statistic and t-statistic were less than the significance level of 0.05, indicating that variance in the annual sediment deposition rate was not assumed to be equal and that the mean was significantly different for the Fangta and Manhonggou watersheds.

The land use change in the Fangta watershed is shown in Figure 5; the main land use type was converted from grassland into forestland, and in 2015, forestland accounted for more than 60% of the area. The arable land and grassland decreased gradually. The arable land area in 1990 was more than 2 times that in 2015. While there was little change in the land use pattern of the Manhonggou watershed, grassland was the most common land use type and accounted for more

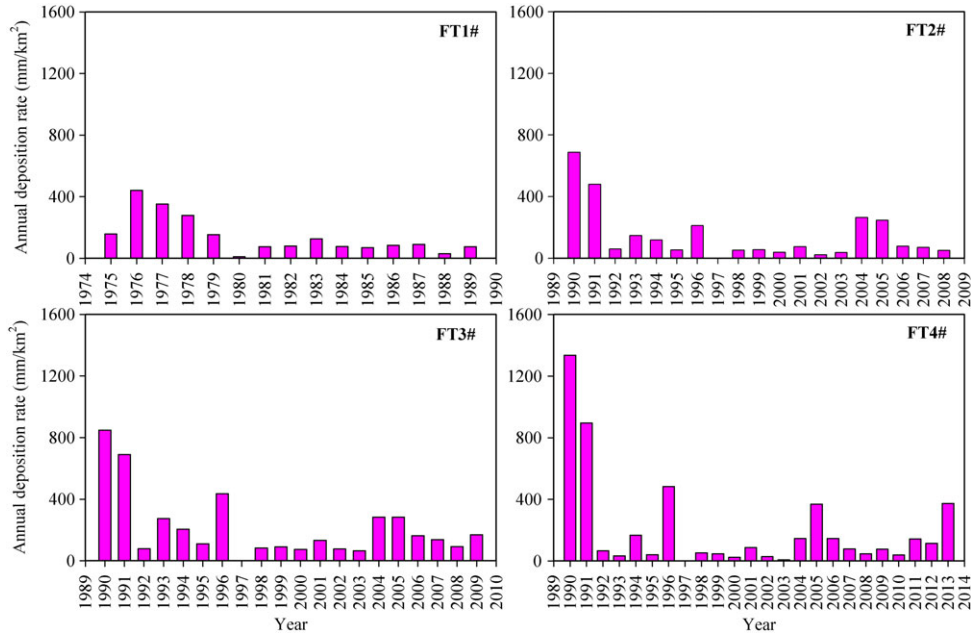


Figure 2. Variations in the annual sediment deposition rate in the Fangta dam-controlled watershed. [Colour figure can be viewed at wileyonlinelibrary.com]

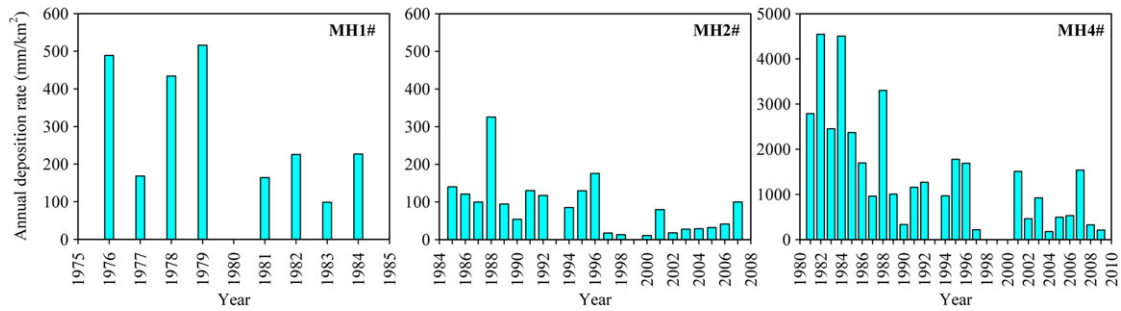


Figure 3. Variations in the annual sediment deposition rate in the Manhonggou dam-controlled watershed. [Colour figure can be viewed at wileyonlinelibrary.com]

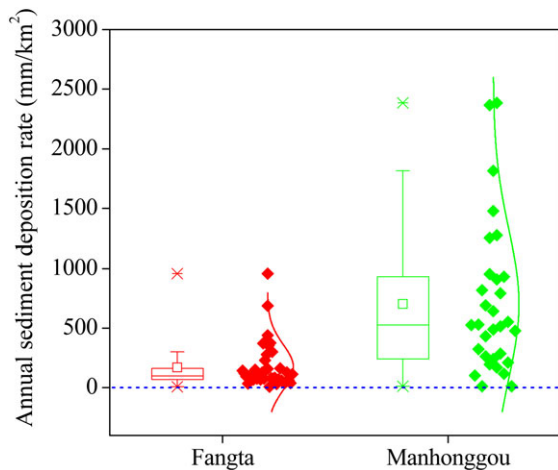


Figure 4. Variations in the annual sediment deposition rate in the small watersheds. A distribution curve is shown to the right side of each box plot, and the data points are represented by diamonds. [Colour figure can be viewed at wileyonlinelibrary.com]

(Figure 6). In this study, the lowest sediment deposition rates in the two small watersheds occurred in the 21st century.

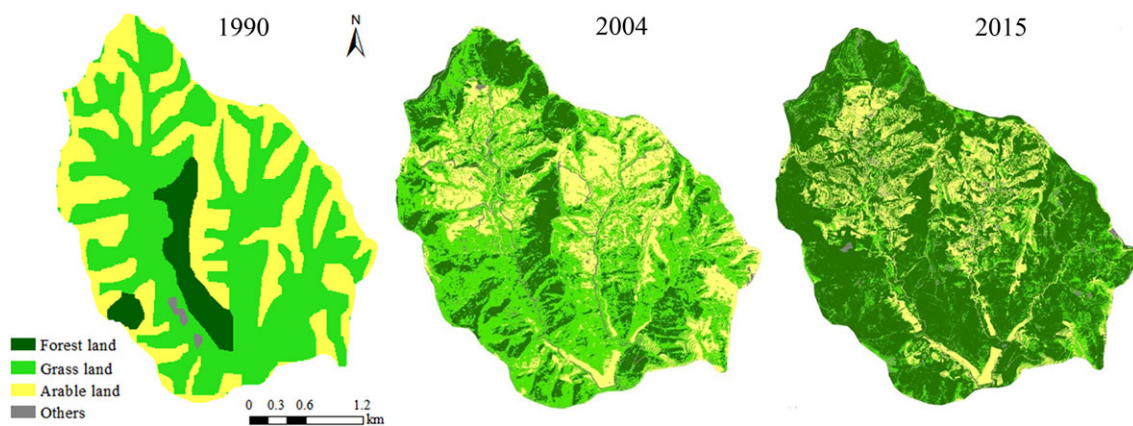
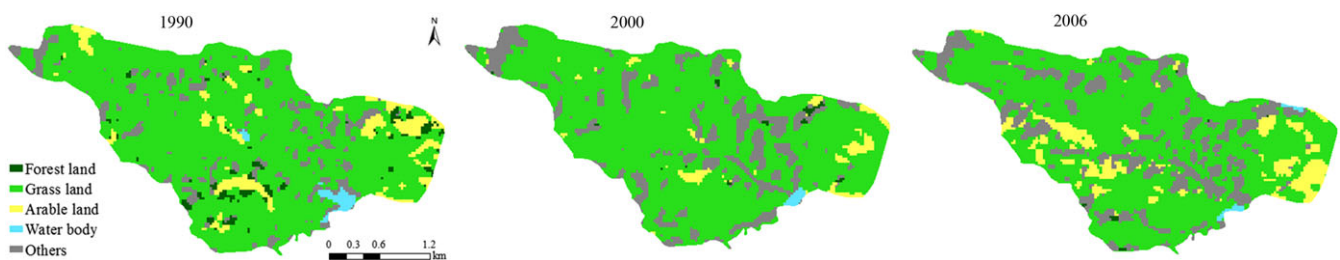
Sediment particle size

The variation in sediment particle size in the Fangta dam-controlled watershed is shown in Figure 7. The average clay (< 0.002 mm), silt (0.002–0.02 mm) and sand (0.02–2 mm) fractions were 6.4%, 36.9% and 56.7% at dam FT1#, 5.9%, 42.9% and 51.2% in FT2#, 9.1%, 53.1% and 37.8% in FT3#, and 6.9%, 43.9% and 49.2% in FT4#, respectively. In general, the soil particle size distribution was centred on the sand and silt fractions. The sand content accounted for approximately 50% of the sediment at dams FT1#, FT2# and FT4#. For a single check-dam, the clay and silt fractions have the same trend from the top to the bottom of the depth profile, while the sand content has the opposite trend. For four check-dams, the silt sediment fraction decreased gradually and the sand content gradually increased from the upstream (dams FT2, FT3, and FT4#) to the downstream (dam FT1#).

In the Manhonggou watershed, the average clay, silt and sand fractions were 6.8%, 59.2% and 34.0% at dam MH1#, 7.2%, 64.4% and 28.4% at dam MH2#, and 5.9%, 58.8% and 35.3% at dam MH4#, respectively (Figure 8). Meanwhile,

Table II. Independent samples t-test of annual sediment deposition rate for the Fangta and Manhonggou watersheds

Small watershed	Mean mm/(km ² ·a)	Std. Deviation	Std. Error	Levene's test		t-test	
				F	Sig.	t	Sig.
Fangta	171.6	191.5	31.1	23.3	0.000	-4.6	0.000
Manhonggou	702.0	624.7	112.2				

**Figure 5.** Land use types of the Fangta watershed in 1990, 2004 and 2015. [Colour figure can be viewed at wileyonlinelibrary.com]**Figure 6.** Land use types of the Manhonggou watershed in 1990, 2000 and 2006. [Colour figure can be viewed at wileyonlinelibrary.com]

the soil particle size distribution was mainly centred on the silt and sand fractions, and the silt content was approximately 60% at dams MH1#, MH2# and MH4#. Similarly, for a single check-dam, the clay and silt fractions have the same trend in change from the top to the bottom of the depth profile, while the sand content has the opposite trend. For three check-dams, the silt sediment fraction decreased gradually and the sand content gradually increased from the upstream (dam MH4#) to the downstream (dam MH1#).

Figure 9 shows the variations in sediment particle size in the two small watersheds; the annual average clay, silt and sand fractions were 6.9%, 42.4% and 50.7% in the Fangta watershed from 1975 to 2013 and 6.5%, 60.6% and 32.9% in the Manhonggou watershed from 1976 to 2009, respectively. Therefore, the clay contents were approximately equal, while the silt and sand contents differed significantly between the two small watersheds. The soil particle size distributions were mainly centred on the sand fraction (50.7%) in the Fangta watershed and silt fraction (60.6%) in the Manhonggou watershed. In Table III, equal variances were not assumed for the clay contents, and the means had no significant difference (F -statistic < 0.05), while equal variances were assumed for the silt and sand contents, and the means had a significant difference because the probabilities of the t -statistic were less than the significance level of 0.05.

Sediment deposition yield

For the Fangta dam-controlled watershed in the loess hilly-gully region, the variation in the annual sediment deposition yield from 1975 to 2013 is shown in Figure 10(a). According to the Mann-Kendall test, the annual sediment deposition yield exhibited a significant decreasing trend ($P < 0.01$), and the annual average sediment deposition yield was 3149.6 t/(km²·a) from 1975 to 2013. In general, the annual average sediment deposition yield decreased gradually from 6090.3 t/(km²·a) in the 1970s to 1683.9 t/(km²·a) in the 1990s and increased slightly to 2376.5 t/(km²·a) after entering the 21st century. According to the Pettitt test, the transition year of the annual sediment deposition yield was determined to be 1991 ($P < 0.05$) (Figure 10(b)). Therefore, we divided the time series (1975–2013) into two stages. In the first stage from 1975 to 1991, the annual average sediment deposition yield was 4894.54 t/(km²·a). The annual average sediment deposition yield in the second stage from 1992 to 2013 was 1801.20 t/(km²·a) (Figure 10(a)). The annual average sediment deposition yield in the second stage decreased more than twice that in the first stage.

For the Manhonggou dam-controlled watershed in the weathered sandstone (*pisha*) region, the annual sediment deposition yield showed a fluctuating decreasing trend from 1976 to 2009

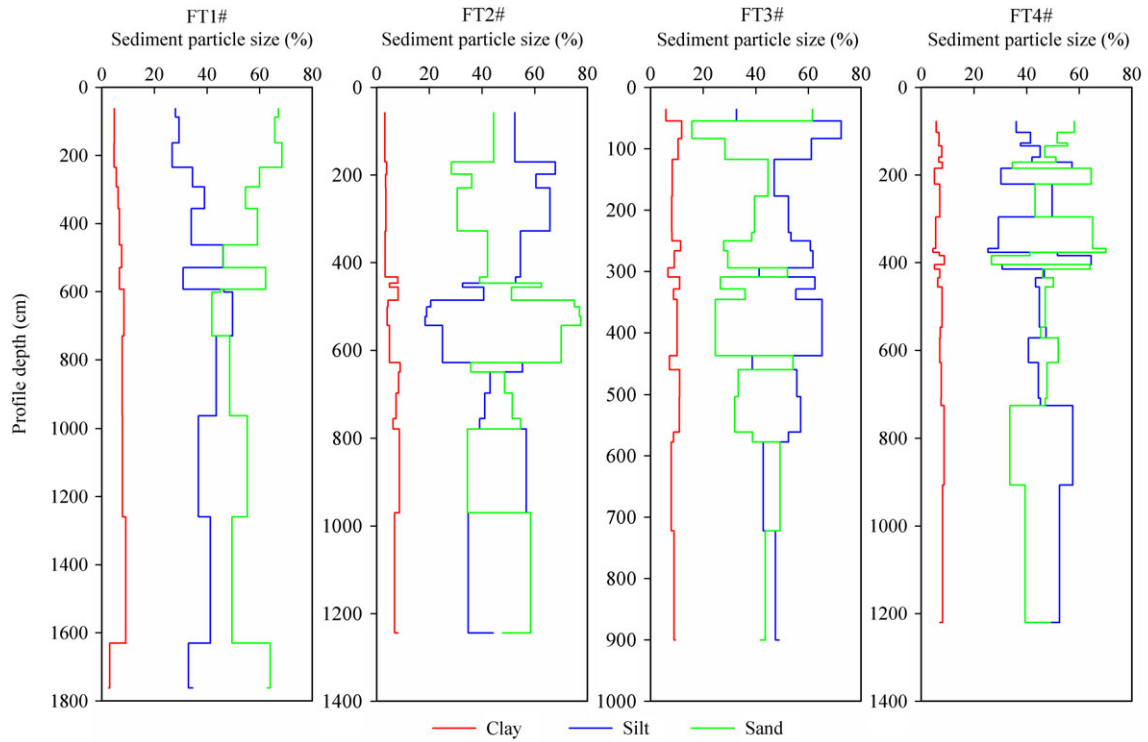


Figure 7. Variations in the sediment particle size in the Fangta dam-controlled watershed. [Colour figure can be viewed at wileyonlinelibrary.com]

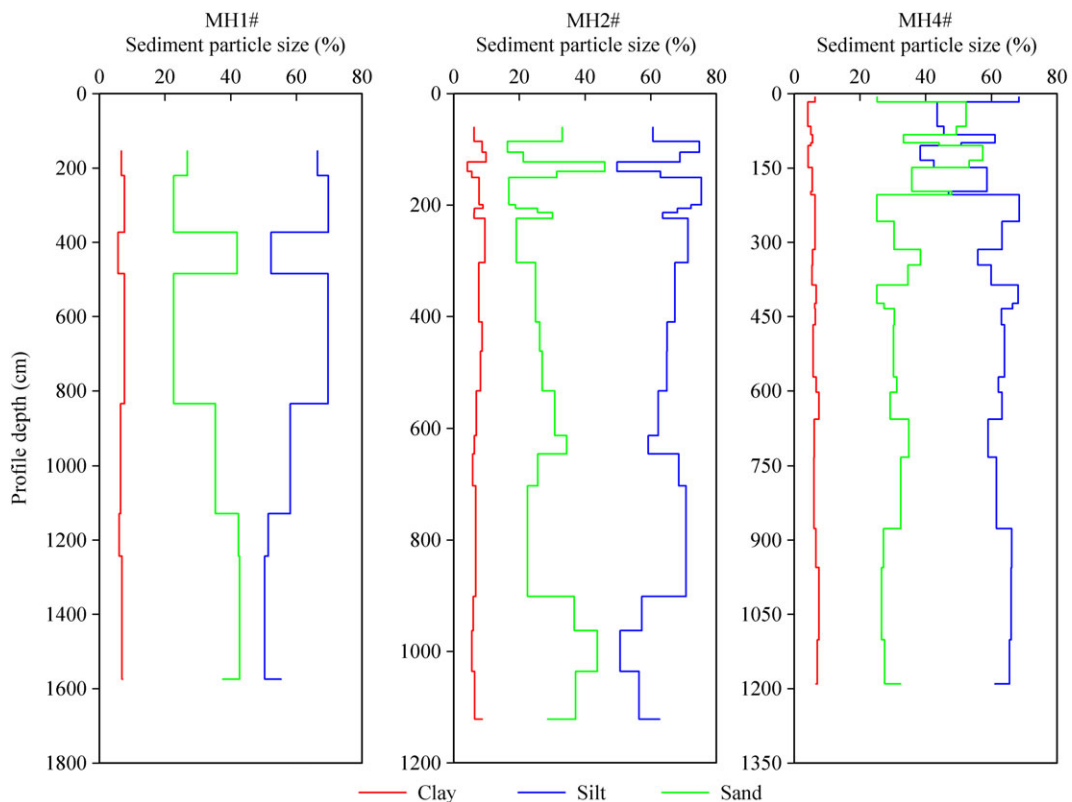


Figure 8. Variations in the sediment particle size in the Manhonggou dam-controlled watershed. [Colour figure can be viewed at wileyonlinelibrary.com]

($P < 0.05$), and the annual average sediment deposition yield was $14011.11 \text{ t}/(\text{km}^2 \cdot \text{a})$ (Figure 10(c)). In the 1970s, the annual average sediment deposition yield was $14938.4 \text{ t}/(\text{km}^2 \cdot \text{a})$. Then, the annual average sediment deposition yield reduced gradually from $15526.1 \text{ t}/(\text{km}^2 \cdot \text{a})$ in the 1980s to $12305.7 \text{ t}/(\text{km}^2 \cdot \text{a})$ in the 21st century. The Pettitt test result of the change point in the

annual sediment deposition yield is shown in Figure 10(d), and the transition year was 1996 in the Manhonggou watershed ($P < 0.05$). The annual average sediment deposition yield in the pre-change period from 1976 to 1996 was $16484.50 \text{ t}/(\text{km}^2 \cdot \text{a})$, while that in the post-change period from 1997 to 2009 was $10015.64 \text{ t}/(\text{km}^2 \cdot \text{a})$ (Figure 10(c)).

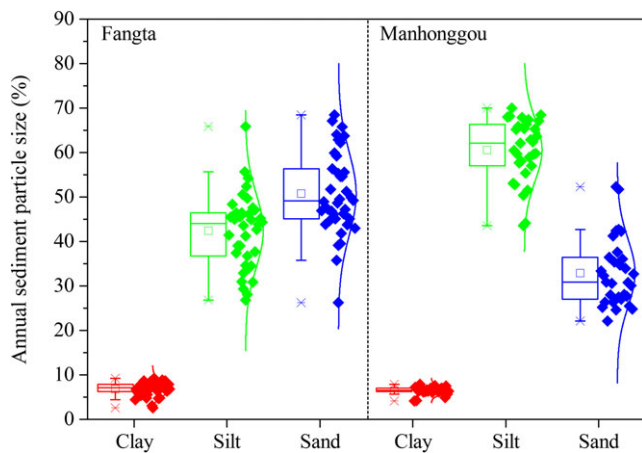


Figure 9. Variations in the sediment particle size in the small watersheds. A distribution curve is shown to the right side of each box plot, and the data points are represented by diamonds. [Colour figure can be viewed at wileyonlinelibrary.com]

In comparison, the annual average sediment deposition yield differed significantly between the two small watersheds, and the annual average sediment deposition yield in the Manhonggou watershed was much larger than that in the Fangta watershed (Figure 11). On the basis of the box plot and the distribution curve, the height of the quartile box for the Manhonggou watershed was higher than that for the Fangta watershed. It was shown that the variation in the annual sediment deposition yield in the Manhonggou watershed was unstable and that the data points were scattered, while the Fangta watershed was relatively stable and concentrated. Table IV showed the independent samples *t*-test of annual sediment deposition yield and the probabilities of the *F*-statistic and *t*-statistic were less than the significance level of 0.05, indicating that equal variances were not assumed for the annual sediment deposition yield and that the means were significantly different in the Fangta and Manhonggou watersheds.

Figure 12 shows the relationship between the annual sediment yield and annual erosive rainfall in the two dam-controlled watersheds. There was a good relationship between these two variables in both the Fangta and Manhonggou watersheds, with high correlation coefficients $R^2 > 0.6$.

Discussion

Sediment yields in the check-dam controlled watersheds

The sediments retained by the check-dams could provide important information on the sediment deposition process, soil erosion evolution and environmental changes in the small

watersheds. Meanwhile, the check-dams in the small watersheds can be used to estimate the specific sediment yield and are important sources of information for contemporary erosion processes at larger spatial and temporal scales. Numerous studies have shown that check-dams or reservoirs typically trap $> 90\%$ of the sediment inflow (Valero-Garcés *et al.*, 1999; Vörösmarty *et al.*, 2003; Batalla and Vericat, 2011; Díaz *et al.*, 2014; García-Ruiz *et al.*, 2015; Mekonnen *et al.*, 2015). Therefore, the sediment deposition at check-dams can represent the majority of the total amount of eroded sediment within the watershed, although some sediment deposition occurs before reaching the check-dams and sediment transport also occurs through the spillways.

The related studies on the specific sediment yield deduced from check-dams in small watersheds on the Loess Plateau are shown in Table V. In the loess hilly-gully region, the specific sediment yields were $4052.1 \text{ t}/(\text{km}^2 \cdot \text{a})$, $4140.0 \text{ t}/(\text{km}^2 \cdot \text{a})$ and $5240.0 \text{ t}/(\text{km}^2 \cdot \text{a})$ at the Yangjuangou, Nianzhuanggou and Beitaigou watersheds of the Yanhe watershed and its surrounding area (Li and Bai, 2003; Wang *et al.*, 2009b; Liu *et al.*, 2015b); these results are close to the annual average sediment yield of $5111.6 \text{ t}/(\text{km}^2 \cdot \text{a})$ at dam FT1# from 1975 to 1989. At dam FT2#, the annual average sediment yield of $726.5 \text{ t}/(\text{km}^2 \cdot \text{a})$ from 1990 to 2008 was close to the annual specific sediment yields of $650.0 \text{ t}/(\text{km}^2 \cdot \text{a})$ and $600.0 \text{ t}/(\text{km}^2 \cdot \text{a})$ at the Beitaliang and Haojialiang watersheds (Liu *et al.*, 2015a, b). In addition, the annual average sediment yields of $1923.4 \text{ t}/(\text{km}^2 \cdot \text{a})$ at dam FT3# from 1990 to 2009 and $2701.3 \text{ t}/(\text{km}^2 \cdot \text{a})$ at dam FT4# from 1990 to 2013 was similar to the annual specific sediment yields of $1967.3 \text{ t}/(\text{km}^2 \cdot \text{a})$ and $2504.0 \text{ t}/(\text{km}^2 \cdot \text{a})$ at the Zhangyinshuiku and Xialaozhuang watersheds, respectively (Zhu *et al.*, 2012). However, in the weathered sandstone (*pisha*) region, the annual average sediment yield of $10728.6 \text{ t}/(\text{km}^2 \cdot \text{a})$ at dam MH1# from 1976 to 1984 was close to the annual specific sediment yields of $10371.0 \text{ t}/(\text{km}^2 \cdot \text{a})$, $10839.1 \text{ t}/(\text{km}^2 \cdot \text{a})$ and $10610.0 \text{ t}/(\text{km}^2 \cdot \text{a})$ at the Weijiata, Wangmaogou and Yangjiagou watersheds of the Huangfuchuan watershed and its surrounding area (Ye *et al.*, 2006; Xue *et al.*, 2011; Zhao *et al.*, 2017b). At dam MH2#, the annual average sediment yield was $12662.9 \text{ t}/(\text{km}^2 \cdot \text{a})$ from 1985 to 2007, which was similar to the annual specific sediment yields of $12702.0 \text{ t}/(\text{km}^2 \cdot \text{a})$ and $13440.0 \text{ t}/(\text{km}^2 \cdot \text{a})$ at the Guandigou watershed and $13577.0 \text{ t}/(\text{km}^2 \cdot \text{a})$ at the Longtuo watershed (Li *et al.*, 2008; Liu *et al.*, 2015a). The annual specific sediment yields of $16931.0 \text{ t}/(\text{km}^2 \cdot \text{a})$, $16812.0 \text{ t}/(\text{km}^2 \cdot \text{a})$ and $17187.5 \text{ t}/(\text{km}^2 \cdot \text{a})$ at the Fenglimao, Huangcaoliang and Xiaoshilata watersheds were close to the annual average sediment yield of $16753.3 \text{ t}/(\text{km}^2 \cdot \text{a})$ at dam MH4# from 1981 to 2009 (Liu *et al.*, 2015a; Zhao *et al.*, 2015). Our results of the sediment deposition yield estimation in the small watersheds were consistent with those of other studies in similar regions.

In the midwestern United States, the maximum soil loss tolerance of deep fertile loamy soil is $600\text{--}1100 \text{ t}/(\text{km}^2 \cdot \text{a})$ (Zhang *et al.*, 2007). In the Loess Plateau region of China, the

Table III. Independent samples *t*-test of the sediment particle size for the Fangta and Manhonggou watersheds

Sediment particle size	Small watershed	Mean (%)	Std. Deviation	Std. Error	Levene's test		t-test	
					F	Sig.	t	Sig.
Clay	Fangta	6.86	1.59	0.26	11.0	0.001	1.2	0.221
	Manhonggou	6.49	0.86	0.15				
Silt	Fangta	42.41	8.29	1.35	0.7	0.415	-9.7	0.000
	Manhonggou	60.58	7.02	1.26				
Sand	Fangta	50.73	9.34	1.51	1.4	0.238	8.5	0.000
	Manhonggou	32.93	7.62	1.37				

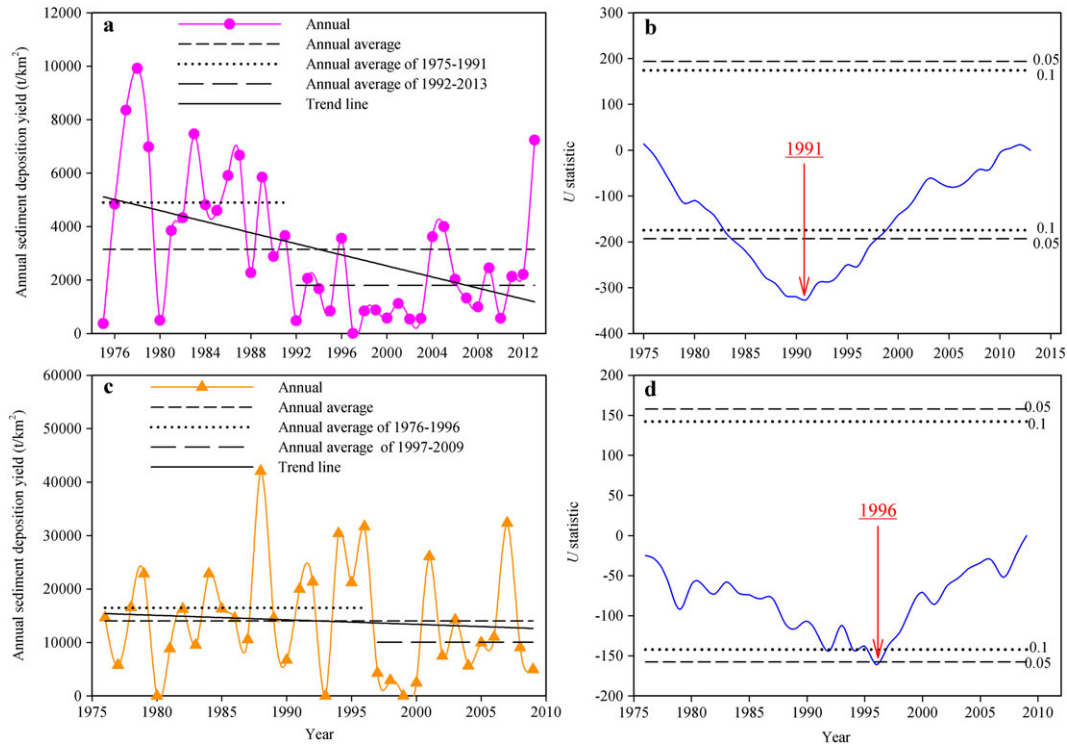


Figure 10. Annual sediment deposition yield and abrupt change years in the Fangta and Manhonggou watersheds (a, b: the Fangta watershed; c, d: the Manhonggou watershed). [Colour figure can be viewed at wileyonlinelibrary.com]

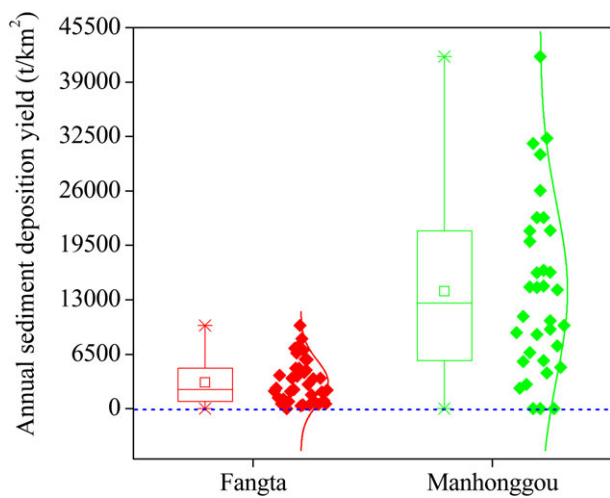


Figure 11. Variations in the annual sediment deposition yield in the small watersheds. A distribution curve is shown to the right side of each box plot, and the data points are represented by diamonds. [Colour figure can be viewed at wileyonlinelibrary.com]

soil loss tolerance is 1000 t/(km²·a) according to the standards for classification and gradation of soil erosion (Ministry of Water Resources, 2008). As previously mentioned, the annual average sediment deposition yield varied greatly between the Fangta (3149.6 t/(km²·a)) and Manhonggou (14011.1 t/(km²·a)) watersheds; these yields were considerably greater than the

tolerable erosion rate and belong to the moderate soil erosion and the extremely intense erosion categories, respectively. In the 21st century, the annual average sediment deposition yield in the Fangta watershed decreased from 3740.53 t/(km²·a) in 1975–1999 to 2094.31 t/(km²·a) in 2000–2013, while that in the Manhonggou watershed decreased from 14721.72 t/(km²·a) in 1976–1999 to 12305.65 t/(km²·a) in 2000–2009. Therefore, soil loss is still a major ecological problem in the Loess Plateau. Considerable efforts are still needed to enhance the vegetation restoration, especially in the areas suffering from intense soil loss.

Influence of the rainfall on the sediment yield

Precipitation has been recognized as one of the main factors driving soil erosion and sediment yield, and its spatial and temporal variability is recognized as one of the main reasons for spatial and temporal variability in the soil erosion (Nadal-Romero *et al.*, 2015). Meanwhile, the annual rainfall has a positive effect on the sediment yield, which is clearly related to sediment detachment and runoff generation (Bellin *et al.*, 2011). In the Chinese Loess Plateau, soil erosion is generally caused by heavy rain or thunderstorms (Wang *et al.*, 2016). Wang and Jiao (1996) also reported that soil erosion is not caused by all rainstorms and that 70% of the intense soil erosion on the Loess Plateau was caused by local rainstorms with short durations and high intensities. Zhao *et al.* (2017b)

Table IV. Independent samples t-test of annual sediment deposition yield for the Fangta and Manhonggou watersheds

Small watershed	Mean t/(km ² ·a)	Std. Deviation	Std. Error	Levene's test		t-test	
				F	Sig.	t	Sig.
Fangta	3149.6	2593.8	415.3	35.7	0.000	-6.0	0.000
Manhonggou	14011.1	10335.7	1772.6				

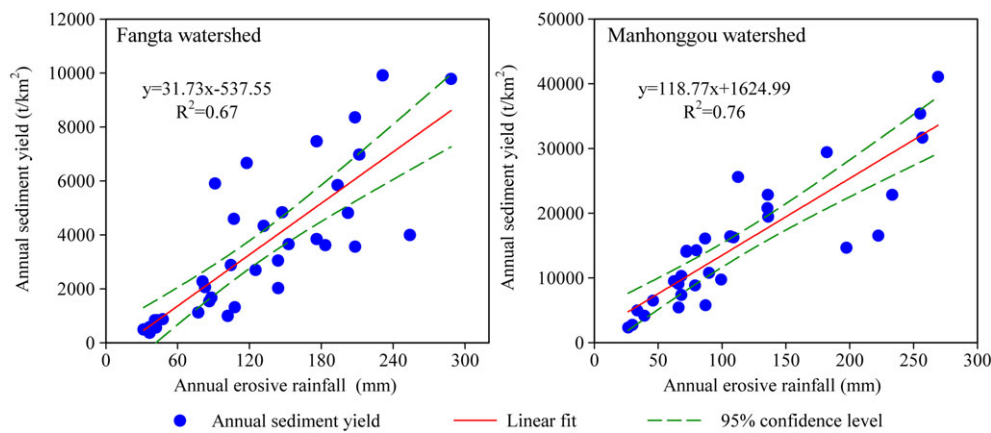


Figure 12. Relationship between the annual sediment yield and annual erosive rainfall in the two dam-controlled watersheds. [Colour figure can be viewed at wileyonlinelibrary.com]

reported similar results and found a close relationship ($R^2 > 0.5$) between the sediment yield and rainfall in the two small watersheds in the Huangfuchuan watershed. Zhang *et al.* (2006) indicated that there was a fairly good relationship ($R^2 > 0.5$, $P = 0.001$) between the specific sediment yield and the annual precipitation of the Yuntaishan watershed in the Yanhe watershed.

However, not all rainfall causes soil erosion. Soil erosion will occur when the rainfall reaches a certain threshold. Moreover, the rainstorms and high specific sediment yield behind the check-dams are generally synchronous. During the erosive rainfall events with rainfall ≥ 12 mm (Xie *et al.*, 2000), soil erosion occurred; however, no sediment was transported to the dams during smaller rainfall events. In this study, the erosive rainfalls necessary for sediment to be deposited at the dams were greater than 30 mm in the Fangta watershed and 20 mm in the Manhonggou watershed. Wang *et al.* (2014) selected a daily precipitation greater than 30 mm to serve as the threshold for erosive rainfall in the Yangjuangou watershed of the Yanhe River. Meanwhile, the threshold for erosive rainfall was greater than 20 mm in the Xiaoshilata watershed of the Huangfuchuan River (Zhao *et al.*, 2015). In the 1970s, the annual erosive rainfall for the sediment yield was 231.1 mm in the Fangta watershed in 1978 and 233.2 mm in the Manhonggou watershed in 1979, while the annual sediment yield was 9913.6 t/(km²·a) and 22821.2 t/(km²·a), respectively. In the 1980s, the annual

erosive rainfall that generated the sediment yield was 131.8 mm in the Fangta watershed in 1982 and 135.8 mm in the Manhonggou watershed in 1984, while the annual sediment yield was 4329.9 t/(km²·a) and 22836.2 t/(km²·a), respectively. In the 1990s, the annual erosive rainfall that generated the sediment yield was 104.3 mm in the Fangta watershed in 1990 and 106.4 mm in the Manhonggou watershed in 1996, while the annual sediment yield was 2879.4 t/(km²·a) and 30364.4 t/(km²·a), respectively. In the 21st century, the annual erosive rainfall that generated the sediment yield was 254.0 mm in the Fangta watershed in 2005 and 256.8 mm in the Manhonggou watershed in 2007, while the annual sediment yield was 3994.0 t/(km²·a) and 32311.8 t/(km²·a), respectively. Hence, the annual sediment yield of the Manhonggou watershed was 2–10 times that of the Fangta watershed from the 1970s to the early 21st century under the same rainfall conditions. A total of 265 and 187 rainfall events greater than 20 mm occurred in the Fangta and Manhonggou watersheds from 1975 to 2013, an average of 6.8 and 4.8 events annually, respectively. Meanwhile, the annual average erosive rainfall was 121.3 mm/a in the Fangta watershed and 113.6 mm/a in the Manhonggou watershed. In contrast, the rainfall frequency and amount in the Fangta watershed were higher than those in the Manhonggou watershed, while the annual average sediment yield in the Fangta watershed (3149.6 t/(km²·a)) was far less than that in the Manhonggou watershed (14011.1 t/

Table V. Related researches of specific sediment yield for check-dams in small watersheds on the Loess Plateau

Study area	Small watershed	Operation period	Dam-controlled area (km ²)	Total deposit mass (t)	Specific sediment yield (t/(km ² ·a))	Reference
Yanhe watershed and its surroundings	Yangjuangou	1979–2004	2.000	202604.0	4052.1	(Wang <i>et al.</i> , 2009b)
	Nianzhuanggou	1976–1984	6.280	234000.0	4140.0	(Li and Bai, 2003)
	Beitaliang	1962–1976	0.200	15484.2	5240.0	(Liu <i>et al.</i> , 2015a, b)
		1999–2012	0.200	1792.7	650.0	
	Haojialiang	2006–2013	2.690	11298.0	600.0	
Huangfuchuan watershed and its surroundings	Zhangyinshuiku	2007–2010	12.500	73773.0	1967.3	(Zhu <i>et al.</i> , 2012)
	Xialaozhuang	2005–2010	3.800	47576.0	2504.0	
	Weijiata	early 70s	4.016	458165.6	10371.0	(Ye <i>et al.</i> , 2006)
	Wangmaogou	1957–1990	0.181	66703.6	10839.1	(Xue <i>et al.</i> , 2011)
	Yangjiagou	2007–2011	0.680	33800.0	10610.0	(Zhao <i>et al.</i> , 2017b)
Huangfuchuan watershed and its surroundings	Guandigou	1979–1987	0.045	5095.2	12702.0	(Li <i>et al.</i> , 2008)
		1964–1978	0.045	8386.3	13440.0	
	Longtou	2005–2012	5.500	597388.0	13577.0	(Liu <i>et al.</i> , 2015a)
	Fenglimao	2005–2012	3.600	487612.8	16931.0	
	Huangcaoliang	2006–2012	3.150	370704.6	16812.0	
	Xiaoshilata	1958–1972	0.640	165000.0	17187.5	(Zhao <i>et al.</i> , 2015)

($\text{km}^2\cdot\text{a}$). As a result, the rainfall was not the main reason for the variation in sediment yield, and it may be largely due to the considerable differences in the underlying surface and soil composition between the two small watersheds.

Effect of the underlying surface on the sediment yield

Soil particle size distribution is one of the most important physical attributes due to its great influence on soil erosion and water movement (Wang *et al.*, 2008). Knowledge of the particle size distribution within the sediment profile is helpful to interpret the past depositional processes and environmental changes (Ritchie and McHenry, 1990; Beierle *et al.*, 2002). Wang *et al.* (2014) indicated that check-dam sediments could be important indicators of environmental change, and the grain size of check-dam sediments is closely influenced by the land use, rainfall event sizes, and sediment deposition processes. In addition, variations in the hydrodynamic conditions can result in different sediment fraction distributions in different parts of the check-dam (Chen *et al.*, 2016). In our study, the soil particle size distribution was centred on the silt and sand fractions (> 90%). The sand fraction in the Fangta watershed accounted for 50.7% of the sediment, and the silt fraction in the Manhonggou watershed accounted for 60.6% of the sediment. Young (1980) indicated that the soil erosion process was selective; particles in the silt-size range are eroded more easily than clay or sand-size particles are eroded. Moreover, the weathered sandstone (*pisha*) had higher runoff and sediment yields than those of the loess soil and the aeolian sandy soil (Tang *et al.*, 2001). Hence, the annual average sediment deposition rate and sediment deposition yield in the Manhonggou watershed were much larger than those in the Fangta watershed.

Furthermore, land cover patterns, soil erosion and sediment yield in the watersheds are closely related. It is widely reported that land use changes may have a tremendous effect on soil loss rates due to sheet and rill erosion at the hillslope scale (Vanmaercke *et al.*, 2012). At the watershed scale, vegetation helps reduce the sediment yield simply by reducing the runoff volume, leading to a sediment reduction rate close to the runoff reduction rate (Zheng *et al.*, 2007). Shi *et al.* (2013) indicated that the landscape characteristics of watersheds could account for as much as 65% and 74% of the variation in the soil erosion and sediment yield, respectively, in the Yangtze River. Jia *et al.* (2012) demonstrated that vegetation cover affects the soil erosion rate, which was inversely proportional to the degree of vegetation cover. The relationships identified between soil erosion and sediment yield and vegetation cover indicated that the vegetation status has a significant impact on sediment formation and transport (Ouyang *et al.*, 2010).

By reasonable adjustment to the land use structure, the benefit in terms of sediment reduction was higher than 80%, and the coverage of permanent vegetation at 61.03% successfully controlled soil and water loss in the Yangou watershed of the Yanhe River (Xu and Tang, 2009). An increase in grassland and forestland by 42%, and a corresponding decrease in farmland by 46%, reduced sediment production by 31% in the Yangjuangou catchment of the Yanhe River (Li *et al.*, 2003). Land use changes alone reduced sediment yield by up to 14%, but in combination with check-dams, the reduction in the sediment yield reached $44 \pm 6\%$ in the Upper Taibilla catchment in southeast Spain (Quiñonero-Rubio *et al.*, 2016). Likewise, in the Saldaña badlands of Spain, check-dams and forest buffers restored at lower elevations effectively reduce

the sediment yield into the Carrión River by nearly three orders of magnitude ($<10^2 \text{ mg L}^{-1}$), compared with the sediment yield data from the 1930s and 1940s ($>10^5 \text{ mg L}^{-1}$) (Navarro-Hevia *et al.*, 2014). Due to the comprehensive effects of slope restoration and gully control, the amount of sediment transported to the check-dams decreased gradually with time. The annual average sediment deposition rate in the Fangta watershed of the Yanhe River decreased from $288.6 \text{ mm}/(\text{km}^2\cdot\text{a})$ in the 1990s to $130.5 \text{ mm}/(\text{km}^2\cdot\text{a})$ in the 21st century. In addition, to convert the croplands to forests and grasslands with the aim of controlling soil erosion and restoring vegetation on the Loess Plateau, the 'Grain for Green' policy was issued by the Chinese Central Government in 1999. It was found that the grassland and forestland were more effective than orchards at reducing gully erosion, and the conversion of sloping farmland to grassland or woodland could reduce gully erosion by more than 90% in the Northern Loess Plateau (Wang *et al.*, 2016). The vegetation restoration program was the main driving factor of the land use change. Wang *et al.* (2009a) also indicated that the conversion of farmland to forestland or grassland was the main reason for the alleviation of soil erosion in the Yanhe River Basin.

In the Huangfuchuan watershed on the Loess Plateau, land use changes between 1980 and 2005 decreased sediment yield by 40.6%, while the land use changes in combination with check-dam construction in 2006 reduced sediment yield by approximately 80% (Zhao *et al.*, 2017a). However, land use changes are long-term sustained sediment control measures at the source, while check-dams have a considerable influence on controlling the sediment yield in the short term by intercepting sediment from the upper area of the watersheds (Boix-Fayos *et al.*, 2008; Quiñonero-Rubio *et al.*, 2016). At present, land use optimization at the small watershed scale is the key measure to control soil erosion, restore the eco-environment and improve the living standard of farmers on the Loess Plateau (Xu and Tang, 2009). Therefore, small catchment management should adhere to the principle of simultaneous control of hillslope and gully and combine biological measures with engineering measures (Chen and Cai, 2006). Zuo *et al.* (2016) reported that grassland was the most common and uniformly distributed land use type in the Huangfuchuan watershed from 1980 and 2005. With the change in land use pattern, the annual average sediment deposition rate in the Manhonggou watershed decreased from $508.7 \text{ mm}/(\text{km}^2\cdot\text{a})$ in the 1990s to $352.2 \text{ mm}/(\text{km}^2\cdot\text{a})$ in the 21st century. Zhao *et al.* (2017b) suggested that the weathered sandstone and bare land contributed 61.5% and 32.5% of the total sediment in the Xiaoshilata watershed and 66.8% and 17.5% of the total sediment in the Yangjiagou watershed in the Huangfuchuan tributary, respectively. Due to the high proportion of weathered sandstone and sandy land and the increase in arable land in the Huangfuchuan watershed, the annual modulus of soil erosion was higher than the permissible value, possibly creating an insecure ecological environment (Yu *et al.*, 2006). Hence, the weathered sandstone and bare land were the main factors for the high sediment yield in the Huangfuchuan watershed. Thus, the application of both land use changes and check-dams to control catchment sediment yield was necessary to achieve a sustainable watershed management strategy and to meet the requirement of ecological security in this area.

Conclusion

The annual average sediment deposition rate showed a decreasing trend with time in the loess hilly-gully region and the weathered sandstone hilly-gully region, and the annual

average sediment deposition rate in the weathered sandstone hilly-gully region (702.0 mm/(km²·a)) was much higher than that in the loess hilly-gully region (171.6 mm/(km²·a)). The soil particle size distribution was centred on the sand fraction (50.7%) in the loess hilly-gully region and on the silt fraction (60.6%) in the weathered sandstone hilly-gully region. The annual average sediment deposition yield in the weathered sandstone hilly-gully region (14011.11 t/(km²·a)) was much larger than that in the loess hilly-gully region (3149.6 t/(km²·a)). The erosive rainfalls for sediment deposition at the check-dams were greater than 30 mm in the loess hilly-gully region and 20 mm in the weathered sandstone hilly-gully region. The rainfall was not the main reason for the sediment yield difference between the two regions. The conversion of farmland to forestland or grassland was the main reason for the alleviation of soil erosion in the loess hilly-gully region, while the weathered sandstone and bare land were the main factors controlling the high sediment yield in the weathered sandstone hilly-gully region.

This research presented a case study of the sediment deposition yield behind check-dams in two small watersheds as determined by using the capacity curve, but further study of the trap efficiency of the check-dams and the sediment sources is required. The sediments deposited behind the check-dams were helpful for elucidating the soil erosion evolution in the small ungauged watersheds under different soil erosion conditions and for providing references with which to plan soil and water conservation measures and implement sediment control strategies, particularly in the semi-arid hilly-gully regions.

Acknowledgements—This study was supported by the National Key Research and Development Program of China (No. 2016YFC0501604), the National Science Foundation of China projects (No. 41371280), the Opening Fund of the State Key Laboratory of Soil Erosion and Dryland Farming on the Loess Plateau (A314021402-1809), the National Science Foundation of China (41472156).

References

- Batalla RJ, Vericat D. 2011. An appraisal of the contemporary sediment yield in the Ebro Basin. *Journal of Soils and Sediments* **11**: 1070–1081.
- Beierle BD, Lamoureux SF, Cockburn JMH, Spooner I. 2002. A new method for visualizing sediment particle size distributions. *Journal of Paleolimnology* **27**: 279–283.
- Bellin N, Vanacker V, van Wesemael B, Solé-Benet A, Bakker MM. 2011. Natural and anthropogenic controls on soil erosion in the Internal Betic Cordillera (southeast Spain). *Catena* **87**: 190–200.
- Boix-Fayos C, de Vente J, Martínez-Mena M, Barbera GG, Castillo V. 2008. The impact of land use change and check-dams on catchment sediment yield. *Hydrological Processes* **22**: 4922–4935.
- Carriquiry JD, Sánchez A. 1999. Sedimentation in the Colorado River delta and Upper Gulf of California after nearly a century of discharge loss. *Marine Geology* **158**: 125–145.
- Chakrapani GJ. 2005. Factors controlling variations in river sediment loads. *Current Science* **4**: 569–575.
- Chen F, Zhang F, Fang N, Shi Z. 2016. Sediment source analysis using the fingerprinting method in a small catchment of the Loess Plateau, China. *Journal of Soils and Sediments* **16**: 1655–1669.
- Chen H, Cai Q. 2006. Impact of hillslope vegetation restoration on gully erosion induced sediment yield. *Science in China: Series D Earth Sciences* **49**(2): 176–192.
- Díaz V, Mongil J, Navarro J. 2014. Topographical surveying for improved assessment of sediment retention in check dams applied to a Mediterranean badlands restoration site (Central Spain). *Journal of Soils and Sediments* **14**: 2045–2056.
- de Vente J, Poesen J, Verstraeten G. 2005. The application of semi-quantitative methods and reservoir sedimentation rates for the prediction of basin sediment yield in Spain. *Journal of Hydrology* **305**: 63–86.
- Feng M, Walling DE, Zhang X, Wen A. 2003. A study on responses of soil erosion and sediment yield to closing cultivation on sloping land in a small catchment using 137Cs technique in the Rolling Loess Plateau, China. *Chinese Science Bulletin* **48**: 2094–2101.
- Fu B. 1989. Soil erosion and its control in the Loess Plateau of China. *Soil Use and Management* **5**: 76–82.
- Gao P, Jiang G, Wei Y, Mu X, Wang F, Zhao G. 2015. Streamflow regimes of the Yanhe River under climate and land use change, Loess Plateau, China. *Hydrological Processes* **29**: 2402–2413.
- García-Ruiz JM, Beguería S, Nadal-Romero E, González-Hidalgo JC, Lana-Renault N, Sanjuán Y. 2015. A meta-analysis of soil erosion rates across the world. *Geomorphology* **239**: 160–173.
- Jia YH, Wang ZY, Zheng XM, Han LJ. 2012. Estimation of soil erosion in the Xihanshui River Basin by using 137Cs technique. *International Journal of Sediment Research* **27**: 486–497.
- Jiao JY, Liu YB, Tang KL. 1992. An approach to runoff and sediment generation of gully and intergully land in small watershed. *Journal of Soil and Water Conservation* **6**: 24–28 (in Chinese).
- Jin Z, Cui B, Song Y, Shi W, Wang K, Wang Y. 2012. How many check dams do we need to build on the Loess Plateau? *Environmental Science & Technology* **46**: 8527–8528.
- Jing K. 1986. A study on gully erosion on the Loess Plateau. *Scientia Geographica Sinica* **6**: 340–347 (in Chinese).
- Kendall MG. 1975. *Rank Correlation Measures*. Charles Griffin: London.
- Khafagy AA, Naffaa MG, Fanos AM, Dean RG. 1992. Nearshore coastal changes along the Nile delta shores. *Coastal Engineering* **2013**: 3260–3072.
- Krause AK, Franks SW, Kalma JD, Loughran RJ, Rowan JS. 2003. Multi-parameter fingerprinting of sediment deposition in a small gullied catchment in SE Australia. *Catena* **53**: 327–348.
- Li M, Li Z, Yao W, Liu P. 2009. Estimating the erosion and deposition rates in a small watershed by the 137Cs tracing method. *Applied Radiation and Isotopes* **67**: 362–366.
- Li M, Yang JF, Hou JC, Chen ZY. 2008. Sediment deposition process for a silt dam in a small watershed in Loess Hilly Region. *Transactions of the CSAE* **24**: 64–69 (in Chinese).
- Li XG, Wei X. 2011. Soil erosion analysis of human influence on the controlled basin system of check dams in small watersheds of the Loess Plateau, China. *Expert Systems with Applications* **38**: 4228–4233.
- Li Y, Bai LY. 2003. Variations of sediment and organic carbon storage by check-dams of Chinese Loess Plateau. *Journal of Soil and Water Conservation* **17**: 1–29 (in Chinese).
- Li Y, Poesen J, Yang JC, Fu B, Zhang JH. 2003. Evaluating gully erosion using 137Cs and 210Pb/137Cs ratio in a reservoir catchment. *Soil & Tillage Research* **69**: 107–115.
- Linag ZS, Wu ZR, Noori M, Yang CQ, Yao WY. 2017. A new ecological control method for Pisha sandstone based on hydrophilic polyurethane. *Journal of Arid Land* **9**(5): 790–796.
- Liu C, Sui J, Wang ZY. 2008. Sediment load reduction in Chinese rivers. *International Journal of Sediment Research* **23**: 44–55.
- Liu LF, Jin SQ, Fu M, Wang Z, Wang K. 2015a. Study on the characteristics of erosion and sediment yield in watershed based on sedimentation information of dam land. *Soil and Water Conservation Science Technology in Shanxi* **1**: 10–13 (in Chinese).
- Liu LF, Du FY, Ma N, Ma ZE, Wang HZ. 2015b. Calculation on soil erosion modulus based on sedimentation investigation of check dam in first subdivision of Loess hilly-gully region. *Bulletin of Soil and Water Conservation* **35**: 124–129 (in Chinese).
- Mann HB. 1945. Nonparametric tests against trend. *Econometrica* **13**: 245–259.
- Mekonnen M, Keesstra SD, Baartman JE, Ritsema CJ, Melesse AM. 2015. Evaluating sediment storage dams: structural off-site sediment trapping measures in northwest Ethiopia. *Cuadernos de Investigación Geográfica* **41**: 7–22.
- Mikhailova MV. 2003. Transformation of the Ebro River Delta under the Impact of Intense Human-Induced Reduction of Sediment Runoff. *Water Resources* **30**(4): 409–417.
- Milliman JD, Syvitski JPM. 1992. Geomorphic/Tectonic control of sediment discharge to the ocean: the importance of small mountainous rivers. *Journal of Geology* **100**: 525–544.

- Ministry of Water Resources of PR China. 2008. Standards for classification and gradation of soil erosion. (SL190—2007): 1–20 (in Chinese).
- Mitchell JK, Mostaghimi S, Pound M. 1983. Primary particle and aggregate size distribution of eroded soil from sequenced rainfall events. *Transactions of the ASAE* **26**: 1773–1777.
- Nadal-Romero E, González-Hidalgo JC, Cortesi N, Desir G, Gómez JA, Lasanta T. 2015. Relationship of runoff, erosion and sediment yield to weather types in the Iberian Peninsula. *Geomorphology* **228**: 372–381.
- Navarro-Hevia J, Araújo JC, Mongil-Manso J. 2014. Assessment of 80 years of ancient-badlands restoration in Saldaña, Spain. *Earth Surface Processes and Landforms* **39**(12): 1563–1575.
- Ni HB, Zhang LP, Zhang DR, Wu XY, Fu XT. 2008. Weathering of pisha-sandstones in the wind-water erosion crisscross region on the Loess Plateau. *Journal of Mountain Science* **5**(4): 340–349.
- Onyando JO, Kisoyan P, Chemelil MC. 2005. Estimation of Potential Soil Erosion for River Perkerra Catchment in Kenya. *Water Resources Management* **19**: 133–143.
- Ouyang W, Hao FH, Skidmore AK, Toxopeus AG. 2010. Soil erosion and sediment yield and their relationships with vegetation cover in upper stream of the Yellow River. *Science of the Total Environment* **409**: 396–403.
- Pettitt AN. 1979. A non-parametric approach to the change-point problem. *Journal of Applied Statistics* **28**: 126–135.
- Pham TN, Yang D, Kanae S, Oki T, Musiak K. 2001. Application of RUSLE model on global soil erosion estimate. *Annual Journal of Hydraulic Engineering* **45**: 811–816.
- Pimentel D. 2006. Soil Erosion: A Food and Environmental Threat. *Environment, Development and Sustainability* **8**: 119–137.
- Porto P, Walling DE, Alewell C, Callegari G, Mabit L, Mallimo N. 2014. Use of a 137Cs re-sampling technique to investigate temporal changes in soil erosion and sediment mobilisation for a small forested catchment in southern Italy. *Journal of Environmental Radioactivity* **138**: 137–148.
- Quiñonero-Rubio JM, Nadeu E, Boix-Fayos C, de Vente J. 2016. Evaluation of the effectiveness of forest restoration and check-dams to reduce catchment sediment yield. *Land Degradation & Development* **27**: 1018–1031.
- Ramos-Díez I, Navarro-Hevia J, San Martín Fernández R, Díaz-Gutiérrez V, Mongil-Manso J. 2016a. Evaluating methods to quantify sediment volumes trapped behind check dams, Saldaña badlands (Spain). *International Journal of Sediment Research* **32**: 1–11.
- Ramos-Díez I, Navarro-Hevia J, San Martín Fernández R, Díaz-Gutiérrez V, Mongil-Manso J. 2016b. Analysis of methods to determine the sediment retained by check dams and to estimate erosion rates in badlands. *Environmental Monitoring and Assessment* **405**: 1–14.
- Ritchie JC, McHenry JR. 1990. Application of radioactive fallout cesium-137 for measuring soil erosion and sediment accumulation rates and patterns: a review. *Journal of Environmental Quality* **19**: 215–233.
- Shi H, Shao M. 2000. Soil and water loss from the Loess Plateau in China. *Journal of Arid Environments* **45**: 9–20.
- Shi ZH, Ai L, Li X, Huang XD, Wu GL, Liao W. 2013. Partial least-squares regression for linking land-cover patterns to soil erosion and sediment yield in watersheds. *Journal of Hydrology* **498**: 165–176.
- Shi ZH, Fang NF, Wu FZ, Wang L, Yue BJ, Wu GL. 2012. Soil erosion processes and sediment sorting associated with transport mechanisms on steep slopes. *Journal of Hydrology* **454–455**: 123–130.
- Shit PK, Bhunia GS, Maiti R. 2013. Assessing the performance of check dams to control rill-gully erosion: Small catchment scale study. *International Journal of Current Research* **4**: 899–906.
- SPSS Inc. 2008. Released, SPSS Statistics for Windows, Version 17.0. SPSS Inc, Chicago.
- Sui JY, He Y, Liu C. 2009. Changes in sediment transport in the Kuye River in the Loess Plateau in China. *International Journal of Sediment Research* **24**: 201–213.
- Suif Z, Fleifle A, Yoshimura C, Saavedra O. 2016. Spatio-temporal patterns of soil erosion and suspended sediment dynamics in the Mekong River Basin. *Science of the Total Environment* **568**: 933–945.
- Syvitski JPM. 2003. Supply and flux of sediment along hydrological pathways: research for the 21st century. *Global and Planetary Change* **39**: 1–11.
- Tang Z, Cai Q, Li Z, Zhao H. 2001. Study on interaction among wind erosion, hydraulic erosion and gravity erosion in sediment-rock region of Inner Mongolia. *Journal of Soil and Water Conservation* **15**: 25–29 (in Chinese).
- Tian P, Zhao GJ, Mu XM, Wang F, Gao P, Mi ZJ. 2013. Check dam identification using multisource data and their effects on streamflow and sediment load in a Chinese Loess Plateau catchment. *Journal of Applied Remote Sensing* **7**: 1–13.
- Vaezi AR, Abbasi M, Keesstra S, Cerdà A. 2017. Assessment of soil particle erodibility and sediment trapping using check dams in small semi-arid catchments. *Catena* **157**: 227–240.
- Valentin C, Poesen J, Li Y. 2005. Gully erosion: Impacts, factors and control. *Catena* **63**: 132–153.
- Valero-Garce's BL, Navas A, Mach'in J, Walling D. 1999. Sediment sources and siltation in mountain reservoirs: a case study from the Central Spanish Pyrenees. *Geomorphology* **28**: 23–41.
- Vanmaercke M, Maetens W, Poesen J, Jankauskas B, Jankauskiene G, Verstraeten G. 2012. A comparison of measured catchment sediment yields with measured and predicted hillslope erosion rates in Europe. *Journal of Soils and Sediments* **12**: 586–602.
- Verstraeten G, Poesen J. 2001. Variability of dry sediment bulk density between and within retention ponds and its impact on the calculation of sediment yields. *Earth Surface Processes and Landforms* **26**: 375–394.
- Vörösmarty CJ, Meybeck M, Fekete B, Sharma K, Green P, Syvitski JPM. 2003. Anthropogenic sediment retention: major global impact from registered river impoundments. *Global and Planetary Change* **39**: 169–190.
- Walling DE, Fang D. 2003. Recent trends in the suspended sediment loads of the world's rivers. *Global and Planetary Change* **39**: 111–126.
- Wang B, Yang Q, Liu Z. 2009a. Effect of conversion of farmland to forest or grassland on soil erosion intensity changes in Yanhe River Basin, Loess Plateau of China. *Frontiers of Forestry in China* **4**: 68–74.
- Wang D, Fu B, Zhao W, Hu H, Wang Y. 2008. Multifractal characteristics of soil particle size distribution under different land-use types on the Loess Plateau, China. *Catena* **72**: 29–36.
- Wang H, Yang Z, Saito Y, Liu JP, Sun X, Wang Y. 2007. Stepwise decreases of the Huanghe (Yellow River) sediment load (1950–2005): Impacts of climate change and human activities. *Global and Planetary Change* **57**: 331–354.
- Wang L, Wei S, Horton R, Shao MA. 2011a. Effects of vegetation and slope aspect on water budget in the hill and gully region of the Loess Plateau of China. *Catena* **87**(1): 90–100.
- Wang S, Yan Y, Yan M, Zhao X. 2012. Quantitative estimation of the impact of precipitation and human activities on runoff change of the Huangfuchuan River Basin. *Journal of Geographical Sciences* **22**: 906–918.
- Wang WZ, Jiao JY. 1996. *Rainfall and erosion sediment yield in the Loess Plateau and sediment transportation in the Yellow River Basin*. Science Press: Beijing (in Chinese).
- Wang Y, Chen L, Fu B, Lu Y. 2014. Check dam sediments: an important indicator of the effects of environmental changes on soil erosion in the Loess Plateau in China. *Environmental Monitoring & Assessment* **186**: 4275–4287.
- Wang Y, Fu B, Chen L, Lu Y, Gao Y. 2011b. Check dam in the Loess Plateau of China: engineering for environmental services and food security. *Environmental Science & Technology* **45**: 10298–10299.
- Wang YF, Fu B, Hou FR, Lv YH, Lu X. 2009b. Estimation of sediment volume trapped by check-dam based on differential GPS technique. *Transactions of the CSAE* **25**: 79–83 (in Chinese).
- Wang ZJ, Jiao JY, Rayburg S, Wang QL, Su Y. 2016. Soil erosion resistance of "Grain for Green" vegetation types under extreme rainfall conditions on the Loess Plateau, China. *Catena* **141**: 109–116.
- Wang ZY, Dittich A. 1999. Effect of particle's shape on incipient motion of sediment. *International Journal of Sediment Research* **14**: 179–186.
- Wang ZY, Wu YS. 2001. Sediment-removing capacity and river motion dynamics. *International Journal of Sediment Research* **16**: 105–115.
- Wasson RJ, Caitcheon G, Murray AS, McCulloch M, Quade JAY. 2002. Sourcing sediment using multiple tracers in the catchment of lake Argyle, northwestern Australia. *Environmental Management* **29**: 634–646.

- Wei Y, He Z, Li Y, Jiao J, Zhao G, Mu X. 2017. Sediment yield deduction from check-dams deposition in the weathered sandstone watershed on the North Loess Plateau, China. *Land Degradation & Development* **28**: 217–231.
- Wen A, Zhang X, Walling DE. 1998. A study on soil erosion rates and sediment sources using caesium-137 technique in a small drainage of the Loess hills. *Acta Geographica Sinica* **53**: 124–133 (in Chinese).
- Xie Y, Liu BY, Zhang WB. 2000. Study on standard of erosive rainfall. *Journal of Soil and Water Conservation* **14**: 6–11 (in Chinese).
- Xin Z, Ran L, Lu XX. 2012. Soil erosion control and sediment load reduction in the Loess Plateau: policy perspectives. *International Journal of Water Resources Development* **28**: 325–341.
- Xu J, Hu C, Chen J. 2009a. Effect of suspended sediment grain size on channel sedimentation in the lower Yellow River and some implications. *Science in China Series E: Technological Sciences* **52**: 2330–2339.
- Xu XL. 1987. Study on the incoming water and sediment yield from intergully area and gully area in the Jiuyuan watershed. *Soil and Water Conservation in China* **8**: 23–26 (in Chinese).
- Xu XZ, Zhang HW, Wang GQ, Chen SC, Dang WQ. 2009b. An experimental method to verify soil conservation by check dams on the Loess Plateau, China. *Environmental Monitoring and Assessment* **159**: 293–309.
- Xu Y, Tang Q. 2009. Land use optimization at small watershed scale on the Loess Plateau. *Journal of Geographical Sciences* **19**: 577–586.
- Xu YD, Fu BJ, He CS. 2013. Assessing the hydrological effect of the check dams in the Loess Plateau, China, by model simulations. *Hydrology and Earth System Sciences* **17**: 2185–2193.
- Xu YD, Fu BJ, He CS, Gao GY. 2012. Watershed discretization based on multiple factors and its application in the Chinese Loess Plateau. *Hydrology and Earth System Sciences* **16**: 59–68.
- Xue K, Yang MY, Zhang FB, Sun XJ. 2011. Investigating soil erosion history of a small watershed using sediment couplet in a dam. *Journal of Nuclear Agricultural Sciences* **25**: 0115–0120 (in Chinese).
- Yan QH, Lei TW, Yuan CP, Lei QX, Yang XS, Zhang ML, Su GX, An LP. 2015. Effects of watershed management practices on the relationships among rainfall, runoff, and sediment delivery in the hilly-gully region of the Loess Plateau in China. *Geomorphology* **228**: 735–745.
- Yang FS, Cao MM, Li HE, Wang XH, Bi CF. 2013. Simulation of sediment retention effects of the single seabuckthorn flexible dam in Pisha Sandstone area. *Ecological Engineering* **52**: 228–237.
- Yang MY, Tian JL, Liu PL. 2006. Investigating the spatial distribution of soil erosion and deposition in a small catchment on the Loess Plateau of China, using ¹³⁷Cs. *Soil & Tillage Research* **87**: 186–193.
- Ye H, Shi JS, Hou HB, Shi YC, Cheng YP, Liu CL. 2006. Exploration on the sedimentary sate assessment in silt retention dam based on GIS and GPS. *Acta Geologica Sinica* **80**: 1633–1636 (in Chinese).
- Young RA. 1980. Characteristics of eroded sediment. *Transactions of the ASAE* **23**: 1139–1146.
- YRCC (Yellow River Conservation Committee, Ministry of water resources conservancy, China). 2014. Bulletin of the Yellow River. <http://www.yellowriver.gov.cn/nishagonggao>.
- Yu F, Li X, Chen Y, Wang H, Yang M. 2006. Land use change and soil erosion evaluation in Huangfuchuan Watershed. *Acta Ecologica Sinica* **26**: 1947–1956 (in Chinese).
- Zhang MS, Liu J. 2010. Controlling factors of loess landslides in western China. *Environmental Earth Sciences* **59**: 1671–1680.
- Zhang X, Jiao J, He X, Wen A, He Y, Zhang Y et al. 2007. Soil loss tolerance and reasonable soil loss. *Science of Soil and Water Conservation* **5**: 114–116 (in Chinese).
- Zhang X, Walling DE, Yang Q, He X, Wen Z, Qi Y et al. 2006. ¹³⁷Cs budget during the period of 1960s in a small drainage basin on the Loess Plateau of China. *Journal of Environmental Radioactivity* **86**: 78–91.
- Zhao G, Klink A, Mu X, Wang F, Gao P, Sun W. 2015. Sediment yield estimation in a small watershed on the northern Loess Plateau, China. *Geomorphology* **241**: 343–352.
- Zhao G, Kondolf GM, Mu X, Han M, He Z, Rubin Z et al. 2017a. Sediment yield reduction associated with land use changes and check dams in a catchment of the Loess Plateau, China. *Catena* **148**: 126–137.
- Zhao G, Mu X, Han M, An Z, Gao P, Sun W et al. 2017b. Sediment yield and sources in dam-controlled watersheds on the northern Loess Plateau. *Catena* **149**: 110–119.
- Zheng M, Cai Q, Chen H. 2007. Effect of vegetation on runoff-sediment yield relationship at different spatial scales in hilly areas of the Loess Plateau, North China. *Acta Ecologica Sinica* **27**: 3572–3581.
- Zhu X, Zhang W, Li J. 2012. Estimation of sedimentation in small reservoirs and silt dams of Haoshui watershed. *Bulletin of Soil and Water Conservation* **32**: 196–199 (in Chinese).
- Zuo D, Xu Z, Yao W, Jin S, Xiao P, Ran D. 2016. Assessing the effects of changes in land use and climate on runoff and sediment yields from a watershed in the Loess Plateau of China. *Science of the Total Environment* **544**: 238–250.